TISSUE ENGINEERING: Part A
Volume 21, Numbers 11 and 12, 2015
© Mary Ann Liebert, Inc.
DOI: 10.1089/ten.tea.2014.0591

Cardiomyoblast (H9c2) Differentiation on Tunable Extracellular Matrix Microenvironment

Muhammad Suhaeri, MS,[1,2] Ramesh Subbiah, MS,[1,2] Se Young Van, MS,[1,2] Ping Du, PhD,[1,2] In Gul Kim, PhD,[1] Kangwon Lee, PhD,[1,2] and Kwideok Park, PhD[1,2]

Extracellular matrices (ECM) obtained from *in vitro*-cultured cells have been given much attention, but its application in cardiac tissue engineering is still limited. This study investigates cardiomyogenic potential of fibroblast-derived matrix (FDM) as a novel ECM platform over gelatin or fibronectin, in generating cardiac cell lineages derived from H9c2 cardiomyoblasts. As characterized through SEM and AFM, FDM exhibits unique surface texture and biomechanical property. Immunofluorescence also found fibronectin, collagen, and laminin in the FDM. Cells on FDM showed a more circular shape and slightly less proliferation in a growth medium. After being cultured in a differentiation medium for 7 days, H9c2 cells on FDM differentiated into cardiomyocytes, as identified by stronger positive markers, such as α-actinin and cTnT, along with more elevated gene expression of Myl2 and Tnnt compared to the cells on gelatin and fibronectin. The gap junction protein connexin 43 was also significantly upregulated for the cells differentiated on FDM. A successive work enabled matrix stiffness tunable; FDM crosslinked by 2wt% genipin increased the stiffness up to 8.5 kPa, 100 times harder than that of natural FDM. The gene expression of integrin subunit α5 was significantly more upregulated on FDM than on crosslinked FDM (X-FDM), whereas no difference was observed for β1 expression. Interestingly, X-FDM showed a much greater effect on the cardiomyoblast differentiation into cardiomyocytes over natural one. This study strongly indicates that FDM can be a favorable ECM microenvironment for cardiomyogenesis of H9c2 and that tunable mechanical compliance induced by crosslinking further provides a valuable insight into the role of matrix stiffness on cardiomyogenesis.

Introduction

Regeneration of the function of injured myocardium is one of the critical issues in cardiac tissue engineering. The use of pluripotent stem cell-derived cardiomyocytes for cell transplantation to treat cardiac diseases has been investigated vastly and recognized as a very promising cell source for cardiac cell therapy.[1,2] Significant improvement has been made in regard to the method of cardiomyocyte differentiation, which mostly focused on the treatment of specific growth factors and/or medium supplements during the induction of cardiomyocyte differentiation.[3,4] Another approach in cardiomyocyte differentiation is the utilization of extracellular matrix (ECM). One example is Matrigel, a solubilized protein extracted from mouse sarcoma that could bring high purity and a large yield of cardiomyocytes by using a sandwich of Matrigel to differentiate pluripotent stem cells, highlighting the importance of ECM for cardiomyogenesis.[5]

However, Matrigel itself carries an obvious limitation for clinical applications. In that sense, an ECM-based study of cardiomyocyte differentiation has been barely investigated. Among the main reasons are ineffectiveness and lack of proper materials and tools. It is plausible that ECM-based strategies, including novel materials, micropattern, and 3D architecture, can find a variety of applications in the area of culture platform, maintenance of differentiation, and cell transplantation.

In fact, ECM is a complex network of so many ECM components and others, covering collagens, adhesion molecules, proteoglycans, and even growth factors and cytokines. It is well known that the unique structure of ECM plays a vital role in determining cell adhesion, proliferation, differentiation, polarity, and migration.[6,7] Compared to the conventional ECM materials, such as fibronectin, gelatin, or collagen, there have been growing evidences on the effect of ECM, not only derived from animal tissues but also from *in vitro* grown cells. These ECM materials are decellularized ECMs and there are a wide variety of applications in tissue engineering and stem cell research.[8–11] For example, the application of ECM scaffolds for mesenchymal stem cells (MSCs) where it supported cell adhesion, cell proliferation, production of new ECM and gave a stronger signal for chondrogenesis than conventional pellet culture.[10]

[1]Center for Biomaterials, Korea Institute of Science and Technology, Seoul, Republic of Korea.
[2]Department of Biomedical Engineering, University of Science and Technology, Daejon, Republic of Korea.

The utilization of ECM from *in vitro* cultured cells gives several benefits than the one obtained from animal or human tissues, such as a 2D culture platform for effective MSC expansion *in vitro*, while maintaining their multipotency, production of pathogen-free ECM, and the possibility of combining different types of ECMs from various cell sources,[12] making this cell-derived matrix (CDM) a very promising tool in the field of tissue engineering.

In this work, we have explored the potential application of CDM as an ECM platform for cardiac tissue engineering. Our hypothesis is that the CDM should provide a beneficial microenvironment for cell adhesion, growth, and differentiation, especially in the induction of cardiomyogenic differentiation. In that sense, the fibroblast-derived matrix (FDM) was evaluated for cardiomyogenesis by comparing it against two most common ECM platforms, that is, gelatin and fibronectin.[13–15] The H9c2 cardiomyoblast, a permanent cardiac cell line isolated from the embryonic rat heart tissue that was fully characterized with morphological, biochemical, and electrophysiological features[16] is employed as a model cell in this work. H9c2 can differentiate into skeletal and cardiac myocytes, with the latter induced by supplementation of all-trans-retinoic acid (RA).[17] The ability of H9c2 to differentiate into cardiomyocytes has prompted its use as a differentiation model in several studies.[18–20] The primary interest of this work is to evaluate the potential of CDM, specifically FDM, in cardiac tissue engineering. Biophysical and biochemical properties of FDM were assessed and followed by examination on cell adhesion, proliferation, and differentiation of H9c2 toward cardiomyocytes. Further study deals with a modified FDM; FDM was crosslinked using genipin, a crosslinking agent to match the mechanical compliance of heart tissue. Followed by some characterizations of the modified FDM, the effect of matrix stiffness on cardiomyogenic differentiation was also investigated. We anticipate that this study will significantly advance our understanding regarding H9c2 cardiomyoblast behavior on tunable matrix environments.

Materials and Methods

Preparation of FDM, crosslinked FDM, and ECM-coated substrates

Mouse fibroblasts (NIH3T3) were obtained from ATCC (CRL-1658) and cultured in Dulbecco's modified Eagle's medium (DMEM) supplemented with 10% fetal bovine serum (FBS), 100 U/mL penicillin, and 100 μg/mL streptomycin under a normal culture condition (5% CO_2, 37°C). For FDM preparation, fibroblasts were seeded ($2 \times 10^4/cm^2$) on gelatin-coated glass coverslips for 5 days, washed with phosphate-buffered saline (PBS), and decellularized using 0.25% Triton-X 100 and 50 mM NH_4OH (221228; Sigma). After washed with PBS, they were treated with 50 U/mL DNase I (18047-019; Invitrogen) and 2.5 μL/mL RNase A (12091-039, Invitrogen), and incubated at 37°C for 2 h. After another washing with PBS thrice, the underlying matrix (FDM) was used freshly or kept in PBS at 4°C for no longer than 2 weeks. In addition, crosslinking reaction of FDM using 2% (w/v) genipin (07803021; Wako) was carried out. Briefly, a stock solution of 5% (w/v) genipin was prepared in dimethyl sulfoxide (DMSO) and diluted to 2% with PBS. The genipin solution was added to FDM, incubated at room temperature, and the crosslinked FDM (X-FDM) was then washed five times with PBS. For gelatin- and fibronectin-coated substrates, glass coverslips (18 mm diameter) were coated with gelatin (G-9391; Sigma) and fibronectin (354008, BD Bioscience), respectively. They were placed in a 12-well plate, immersed with 0.5% (w/v) gelatin for 30 min or with 5 μg/cm^2 fibronectin for 1 h, and air-dried before use.

Characterization: AFM, SEM, and immunofluorescence

The surface morphology, topography, and mechanical property of FDM were evaluated by using a Bio-atomic force microscope (AFM, NanoWizard II JPK Instruments) coupled with an inverted optical microscope (Nikon), as described by a previous publication.[21] Briefly, the combined inverted optical stage helped precise lateral positioning of the AFM tip over the region of interest in target materials. The scan size was adjusted to $100 \times 100\ \mu m^2$ to accommodate typical surface features while maintaining a high resolution. CONT-S sphere probes (400 nm radius; Nanoworld Services GmbH) with 0.4 N/m force constant were employed for surface imaging. The data obtained from the Bio-AFM height scale images were used to calculate the surface roughness of materials. Images were processed using JPK software (v3.3.25). Young's modulus (E) of the substrates was also measured through a nanoindentation method using a silicon nitride (Si_3N_4) cantilever (PT.SiO2.AU.SN.5) with the spring constant of 0.01 N/m. The E was subsequently determined by using the Hertz's contact model in JPK data processing software (JPK instruments). For calculation of material stiffness, the poison ratio was assumed 0.5, the ramp size was 1 μm, and the loading speed was 1 μm/s. A series of indentation forces (0.5–10 nN) were tested to calibrate whether the indentation depth was in the proper range between 20–200 nm to prevent substrate surface defects and hertz model limitation.

Meanwhile, for scanning electron microscopy (SEM) analysis, FDM was fixed in 4% formaldehyde for 30 min at room temperature, washed with deionized water (three times), and dried over a series of ethanol gradients. Finally, it was air-dried overnight before sputter coated with platinum and then subjected to the observation under SEM (Phenom G2 Pro Desktop, Phenom World). For immunofluorescence (IFS), FDM was fixed with 4% formaldehyde for 30 min, washed with PBS (3 times), blocked with 1% bovine serum albumin (BSA) for 1 h at room temperature, and then incubated with primary antibodies, mouse anti-fibronectin (SC-8422; Santa Cruz Biotechnology), goat anti-type I collagen (SC-25974; Santa Cruz Biotechnology), and goat anti-laminin (SC-16588; Santa Cruz Biotechnology), respectively, overnight at 4°C. After washed with PBS thrice, they were incubated with secondary antibodies, Alexa Fluor 488-conjugated goat anti-mouse IgG (A11001; Invitrogen) or Alexa Fluor 594-conjugated donkey anti-goat IgG (705-585-003; Jackson Immunoresearch), for 1 h at room temperature. Those samples were rinsed again with PBS and mounted in a mounting medium, with DNA-specific 4′, 6-diamidino-2-phenylindole (DAPI; H1200; Vector Lab.) treatment. Fluorescence was observed using a confocal laser scanning microscope (Olympus Fluo View FV1000).

Cardiomyoblast (H9c2) and primary rat cardiomyocyte cultures

Rat cardiomyoblasts (H9c2) (CRL-1446, ATCC) were seeded (1×10^4 cells/cm^2) and cultured in DMEM. For H9c2 differentiation, they were initially supplemented with 10% FBS (growth medium, GM) for 3 days and switched to the differentiation medium (DM; 1% FBS and 50 nM all-trans-retinoic acid [RA, R2625; Sigma]) for 7 days. RA was added daily in the DM and the medium was changed every other day. Meanwhile, to obtain a positive control of cardiomyoblast differentiation, the heart ventricles of Sprague-Dawley rats (1–3 day-old) were aseptically harvested, washed with Hank's balanced salt solution (24020-117; Gibco), and digested with 100 U/mL collagenase (17101-015; Gibco) solution containing 0.6 mg/mL pancreatin (P3292; Sigma). The isolated cardiac cells were further purified by using a preplating method and cultured in the same condition as described in the GM. The rat cardiomyocytes were identified with an active beating under a microscopic observation.

Cardiomyoblast viability and proliferation assay

Cell viability on different ECM substrates was determined using the LIVE/DEAD Viability/Cytotoxicity Kit (MP03224; Invitrogen) according to the manufacturer's instruction. Briefly, cells (three replicates in each group) were cultured for 1 day before the medium was aspirated, then incubated with the LIVE/DEAD solution for 30 min at 37°C, and mounted on glass coverslip. Live and dead cells were identified in green and red signals, respectively, under a fluorescent microscope (CKX-41, Olympus). For cell proliferation assay, H9c2 were seeded on gelatin- and fibronectin-coated glass coverslips and FDM at a density of 1×10^4 cells/cm^2 ($n = 3$) and cultured in GM for 3 days. The medium was then switched to DM and maintained for another 7 days. Cell proliferation was assessed during cultures in the GM at day 1 and 3 and in the DM at day 3 and 7, respectively, by using the Cell Counting Kit-8 (Dojindo; CK04). Briefly, the CCK-8 solution (100 μL) was added to the media in the culture well (1000 μL) and incubated for 1.5 h at 37°C. After then, 100 μL aliquot of the media was aspirated and used for absorbance reading at 450 nm using Multiskan microplate reader (Thermo Scientific).

IFS of focal adhesion and cardiomyogenic markers

To observe focal adhesion (FA) and evaluation of the differentiation of H9c2 cells into cardiomyocytes, several antibodies were employed for IFS. Briefly, H9c2 cells were washed with PBS, fixed with 4% formaldehyde for 30 min at room temperature, permeabilized with 0.1% Triton-X 100, and blocked with 1% BSA for 1 h at room temperature. For each step, samples were washed thrice with PBS. They were then incubated with primary antibodies overnight at 4°C, washed with PBS, and incubated with secondary antibodies for 1 h at room temperature. Final washing was done before the samples were mounted in a mounting medium with DAPI (H1200; Vector Lab.). Fluorescence image was observed using a microscope or a confocal laser scanning microscope. Rhodamine phalloidin (R415; Life Technology) was used for F-actin staining. Primary antibodies, mouse monoclonal anti-vinculin (sc-73614; Santa Cruz), mouse monoclonal anti-sarcomeric α-actinin (ab9465; abcam), and mouse monoclonal anti-cardiac troponin T (ab8295; abcam), were employed to detect vinculin, sarcomeric α-actinin, and cardiac troponin T (cTnT), respectively, along with the treatment of secondary antibody, Alexa Fluor 488 goat anti-mouse (A11001; Life Technology). Primary antibody rabbit polyclonal anti-connexin 43 (ab11370; abcam) and secondary antibody rhodamine red-X goat anti-rabbit (R6394, Invitrogen) were also administered for a gap junction protein, connexin 43 (Cx43) staining. Meanwhile, quantitative analysis of positive fluorescence signals was carried out using ImageJ software (NIH). Information related to cell morphology, such as cell area and circularity, was assessed by manually drawing cell borders and processing them through ImageJ. Morphological values ranged from 0 (elongated polygon) to 1 (perfect circle). The averages and standard deviations were obtained out of three replicates in each group. Analysis for vinculin staining was carried out by selecting positively stained cells (green). Each experimental group contained three replicates and we randomly selected 20 cells (average six to seven cells per replicate) in total for image analysis. Cardiomyogenic differentiation markers, α-actinin and cTnT, and gap junction protein, Cx43, were also analyzed based on the number of cells positively stained and those numbers were then normalized to the total number of cells in a given area (700×525 μm^2) of each image. Each test group has three replicates and five random images were chosen per replicate and analyzed.

Quantitative PCR: integrin and cardiomyogenic markers

Total RNA was extracted from H9c2 cells ($n = 3$, each group) using TRIzol (15596-026; Life Technology) following the manufacturer's instruction. The concentration and purity of the extracted RNA were determined through the absorbance reading at 260 and 280 nm, respectively, using the Multiskan microplate reader. Afterward, cDNA was synthesized using oligo primer (25081; Intron Biotech.) following the manufacturer's instruction at 45°C for 60 min and the RTase inactivation step at 95°C for 5 min in the PCR instrument (Takara; PCR thermal cycler). The obtained samples were further processed using RealMOD Green Real-time PCR Master mix kit (25343; Intron Biotech.) and then subjected to amplification in a qPCR instrument (Applied Biosystems; Real-Time PCR System 7500). Primers used for integrin expression are as follows: integrin α5 (α5; F-AGTCCTGAAATGCCCTGAAGC, R-GAAGGCTGAA CGGCTGGTAT), integrin β1 (β1; F-CCAAGTGGGAC ACGGGTGAA, R-CTTGGTGTTGCAAACTCCGC), and GAPDH (F-ATGGTGAAGGTCGGTGTAA, R-TCCACAG TCTTCTGAGTGGC). On the other hand, primers for cardiomyogenic markers are selected based on the previous report[20]: actin alpha 1 cardiac muscle (Actc1; F-ATGATGC TCCCAGAGCTGTC, R-TGTCGTCCCAGTTGGTGATA), myosin regulatory light chain 2, ventricular/cardiac isoform (Myl2; F-AAAGAGGCTCCAGGTCCAAAT, R-CCTCTC TGCTTGCGTGGTTA), and cardiac muscle troponin T (Tnnt; F-GCGGAAGAGTGGGAAGAGACA, R-CCACAG CTCCTTGGCCTTCT).

Statistical analysis

All data presented are mean ± standard error. Statistical analysis was performed using GraphPad prism 5 (GraphPad Software, Inc.). One-way ANOVA with a *post hoc* Tukey's multiple comparison test was used for three experimental groups (gelatin, fibronectin, and FDM). Student *t*-test was applied for two test groups (FDM and X-FDM). Statistically significant difference was denoted as *($p < 0.05$), **($p < 0.01$), or ***($p < 0.001$).

Results

Biophysical properties of gelatin, fibronectin, and FDM were analyzed using AFM (Fig. 1A, B). While root mean square (RMS) roughness of gelatin and fibronectin was 14.78 ± 2.25 nm and 8.61 ± 1.32 nm, respectively, that of FDM was 188.24 ± 25.96 nm. This suggests a huge difference of surface topography: both gelatin and fibronectin possess a very smooth surface, but FDM has a much rough one. The matrix stiffness of each substrate was also examined using AFM (Fig. 1C). Fibronectin (266 ± 62 Pa) showed the highest value of Young's modulus in comparison to that of gelatin (176 ± 28 Pa) or FDM (73 ± 29 Pa). Further investigation of the surface texture of FDM exhibits a fibrillar matrix structure as observed through SEM (Fig. 1D). In addition, major components of FDM (fibronectin, collagen I, and laminin) were also identified by means of an immunofluorescent staining (Fig. 1D).

To assess the morphological characteristics of H9c2 cardiomyoblasts on gelatin, fibronectin, and FDM, cells were cultured in the growth medium (GM) or differentiation medium (DM). They were then subjected to F-actin phalloidin staining at GM3 and DM7, respectively. Cell morphology was significantly different from the cells cultured in either the GM or DM condition (Fig. 2A). They showed a polygonal shape in GM but exhibited a highly elongated morphology in DM. From the quantitative analysis, while there was little difference in cell area at GM3, cells on FDM have a much larger area (1693 ± 554.4 μm^2) compared to those on gelatin (1246 ± 369.7 μm^2) at DM7 (Fig. 2B).

Cell circularity exhibited a relatively higher circularity (0.54 ± 0.14) on FDM at GM3 compared to that of gelatin (0.34 ± 0.10) and fibronectin (0.44 ± 0.11) (Fig. 2C). It is interesting that cell circularity significantly reduced when the medium condition was switched to DM7. The percentage of reduction was also notable with FDM compared to that of gelatin. In addition, cell proliferation assay showed that while in GM conditions cell numbers continuously increased with time in all the groups and those in DM conditions revealed a slight or little change with time (Fig. 2D). The cells on FDM showed a relatively lower proliferation activity compared to the other groups in both GM and DM conditions.

Assessment on H9c2 cardiomyoblast differentiation on gene and protein levels was carried out. DM consists of 1% FBS and daily supplementation of 50 nM RA for 7 days. Some of the cell populations were positively stained with cardiac differentiation marker proteins, such as α-actinin and cardiac troponin T (cTnT) (Fig. 3A), along with no positive signals

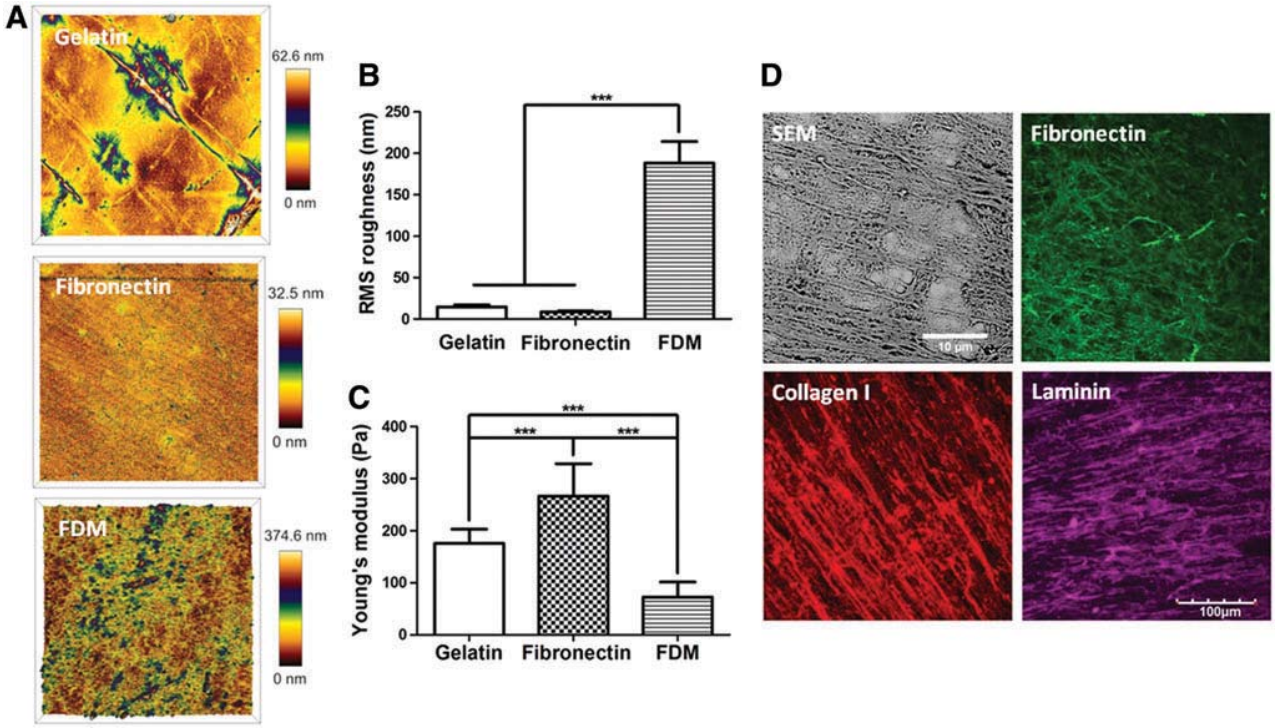

FIG. 1. Characterization of extracellular matrix (ECM) substratum. **(A)** Substrate topography as measured by AFM. The size of AFM image is 100 × 100 μm^2 with color bars on the side. **(B)** Quantitative analysis of root mean square roughness. **(C)** Measurement of substrate stiffness (Young's modulus). **(D)** SEM and immunofluorescence (IFS) images of fibroblast-derived matrix (FDM) showing a fibrillar structure and major ECM proteins. Scale bars for SEM and IFS are 10 μm and 100 μm, respectively. Statistical significance (***$p < 0.001$). Color images available online at www.liebertpub.com/tea

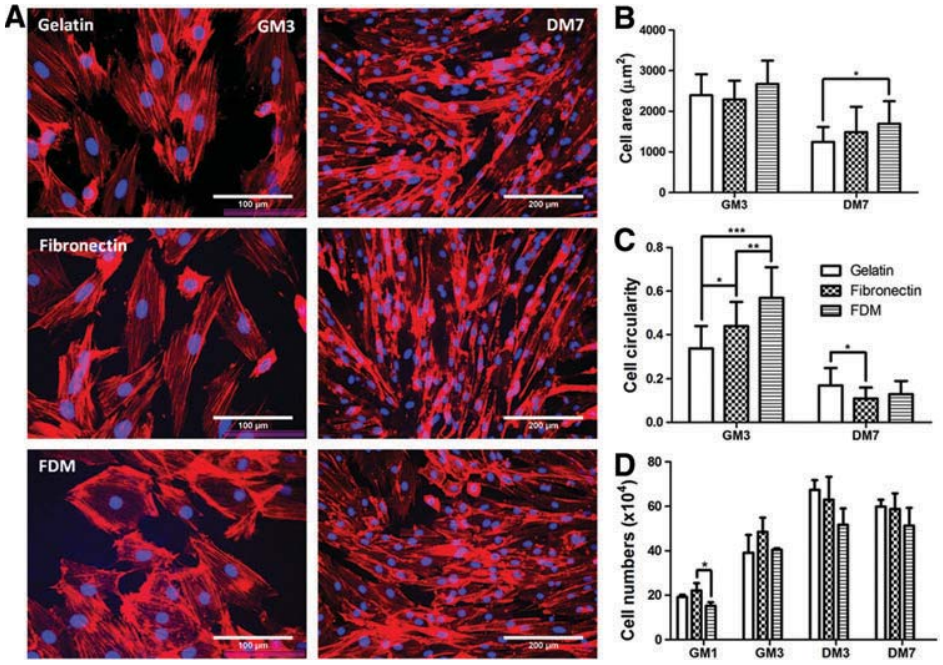

FIG. 2. Comparison of cell morphology, cell area, circularity, and cell numbers of H9c2 cardiomyoblasts in growth medium (GM) and differentiation medium (DM). **(A)** F-actin (*red*) staining of H9c2 cultivated on gelatin, fibronectin, and FDM at GM3 and DM7, respectively, with nuclei stained by DAPI (*blue*). **(B, C)** Quantitative analysis of cell area and circularity at GM3 and DM7 based on IFS image analysis using ImageJ. **(D)** H9c2 proliferation on gelatin, fibronectin, and FDM for specific periods in GM and DM, respectively. Statistical significance ($*p < 0.05$, $**p < 0.01$, and $***p < 0.001$). Color images available online at www.liebertpub.com/tea

for the cells before the induction of differentiation at GM3 (Fig. 3A, insets). The differentiated cardiomyoblasts were morphologically elongated and multinucleated. In addition, when primary neonatal rat cardiomyocytes were also examined with the same markers, they also displayed the same positive signals as identified in the differentiated H9c2 (Fig. 3B). Quantitative analysis of the positive markers was carried out based on the ratio between the number of nuclei positive to cardiac markers and the total number of nuclei (Fig. 3C). Interestingly, FDM exhibited a significantly higher percentage of positive cells compared to that of gelatin or fibronectin; differentiation marker of α-actinin on FDM (31.4% ± 8.30%) is more strongly expressed than gelatin (18.7% ± 8.30%) or fibronectin (12.6% ± 2.15%). Additionally, the protein expression level of cTnT was also greatly improved with FDM (28.2 ± 3.56) compared to that with gelatin (18.1 ± 4.13) or fibronectin (15.9 ± 6.11). Taken together, the cardiomyogenic differentiation efficiency of α-actinin was 1.7- and 2.5-fold

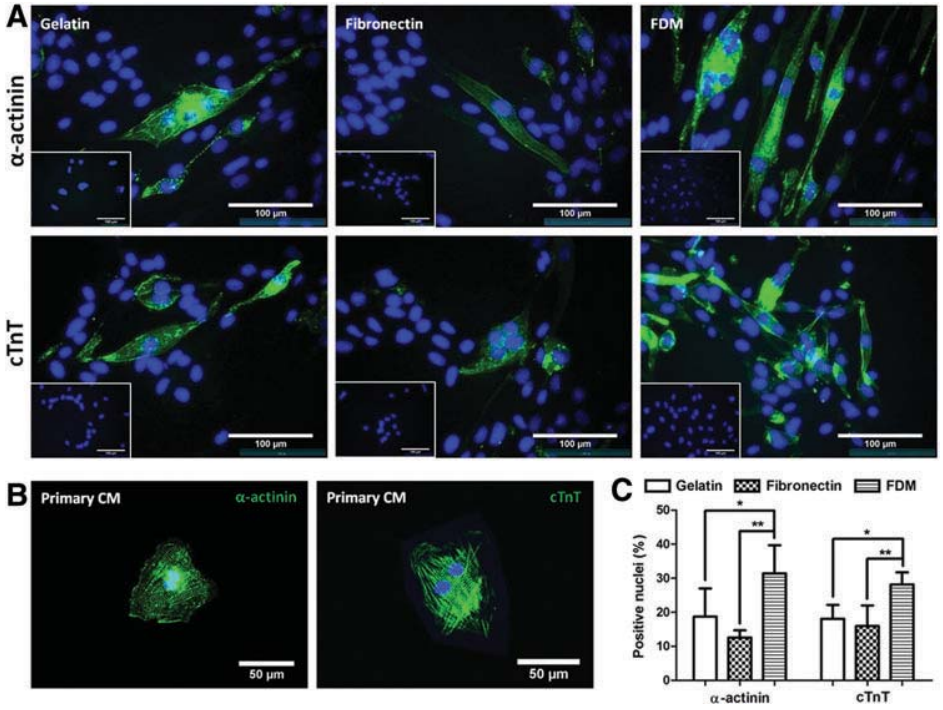

FIG. 3. H9c2 cardiomyoblast differentiation into cardiomyocytes on gelatin, fibronectin, and FDM at DM7. **(A)** IFS of α-actinin and cTnT (both shown in *green*) and nuclei stained with DAPI (*blue*). *Insets* are the cells before the induction of differentiation at GM3. Scale bars in all images (including *insets*) are 100 μm. **(B)** IFS of primary cardiomyocytes (CM) as a positive control stained with α-actinin and cTnT, respectively, and nuclei stained with DAPI (*blue*). Scale bar = 50 μm. **(C)** Quantitative analysis of nuclei positive for α-actinin and cTnT at DM7 based on IFS image analysis using ImageJ. Data collected from five random IFS images. Statistical significance ($*p < 0.05$, $**p < 0.01$). Color images available online at www.liebertpub.com/tea

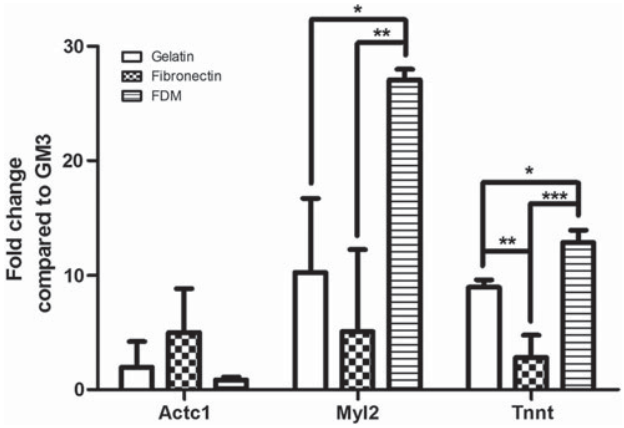

FIG. 4. Relative gene expression level of differentiating H9c2 cardiomyoblasts into cardiomyocytes on gelatin, fibronectin, and FDM at DM7 compared to the one at GM3. Cardiomyogenic marker genes are actin alpha cardiac 1, myosin light chain 2, and cardiac muscle troponin T (Actc1, Myl2, and Tnnt, respectively). Statistical significance (*$p < 0.05$, **$p < 0.01$, and ***$p < 0.001$).

higher with FDM, and similarly, it was 1.6- and 1.8-fold greater for cTnT compared to that of gelatin and fibronectin, respectively.

Cardiomyogenic differentiation of H9c2 was also examined at DM7 through gene expression of some cardiomyogenic markers: actin alpha cardiac 1 (Actc1), myosin light chain 2 (Myl2), and cardiac muscle troponin T (Tnnt). The results presented that H9c2 cells undergoing the differentiation on FDM could be upregulated 2.6- and 5.3-fold more in the expression of Myl2 than on gelatin and fibronectin, respectively (Fig. 4). Another gene expression of Tnnt also elevated significantly 1.4- and 4.6-fold higher on FDM, compared to the two counterpart ECM substrates. The expression of Actc1, however, showed little difference among the test groups. In addition, synthesis of an important maturation marker of cardiomyocytes, connexin 43 (Cx43), a gap junction protein was also monitored. While some cells were Cx43 positive on the given ECM substrates, their intensity and distribution were significantly different among the test groups; FDM held much more Cx43-positive cells, as contrasted with those on gelatin and fibronectin, both at GM3 and DM7 (Fig. 5A). As a positive control, primary neonatal cardiomyocytes were also Cx43 positive (Fig. 5B). Quantitative analysis indicated that percentages of Cx43-positive cells at GM3 were $33.8\% \pm 4.5\%$ (FDM), $22.2\% \pm 7.1\%$ (gelatin), and $18.4\% \pm 3.3\%$ (fibronectin), whereas at DM7 were 48.9 ± 5.8 (FDM), 23.2 ± 11.3 (gelatin), and 34.3 ± 12.4 (fibronectin) (Fig. 5C).

Furthermore, to investigate the effect of matrix stiffness in cardiomyogenic differentiation of H9c2, FDM was subjected to a chemical crosslinking using 2% genipin solution. As a result, crosslinked FDM (X-FDM) exhibited an increased Young's modulus of 8507 ± 1696.4 Pa, significantly larger than that of FDM itself (72 ± 29.1 Pa), as determined by AFM (Fig. 6A). The surface roughness also changed from 188.24 ± 25.96 (FDM) to 336.20 ± 28.92 (X-FDM). Cell viability assay revealed that cells on X-FDM were as comparable in their viability as the one on FDM (Fig. 6B). From the analysis of cell morphology, it was interesting that the cell area on X-FDM increased with time from GM1 to GM3, whereas the cell area on FDM rather decreased in the given time period (Fig. 6C, D). The difference of cell area was insignificant at DM7 between FDM and X-FDM. Assessment of cell circularity demonstrated that there was little difference between them in both the growth and differentiation medium conditions (Fig. 6E). Cell proliferation

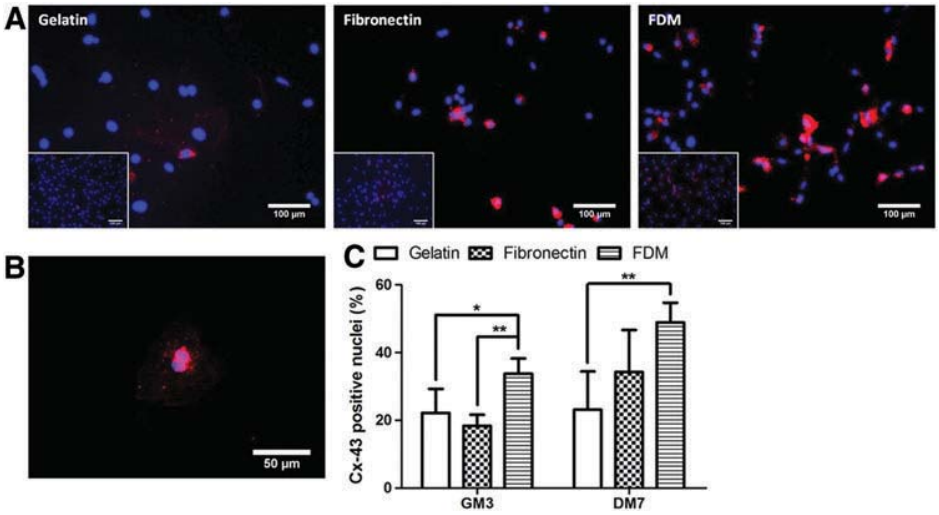

FIG. 5. **(A)** Expression of gap junction protein, connexin 43 (Cx43, *red*) on gelatin, fibronectin, and FDM at DM7. Nuclei are stained with DAPI (*blue*). *Insets* are the cells before the induction of differentiation at GM3. Scale bars = 100 µm. **(B)** IFS of primary cardiomyocytes as a positive control stained with Cx43 and nuclei stained with DAPI (*blue*). Scale bars are 50 µm. **(C)** Quantitative analysis of nuclei positive for Cx43 at GM3 and DM7 based on IFS image analysis using ImageJ. Data collected from five random IFS images. Statistical significance (*$p < 0.05$, **$p < 0.01$). Color images available online at www.liebertpub.com/tea

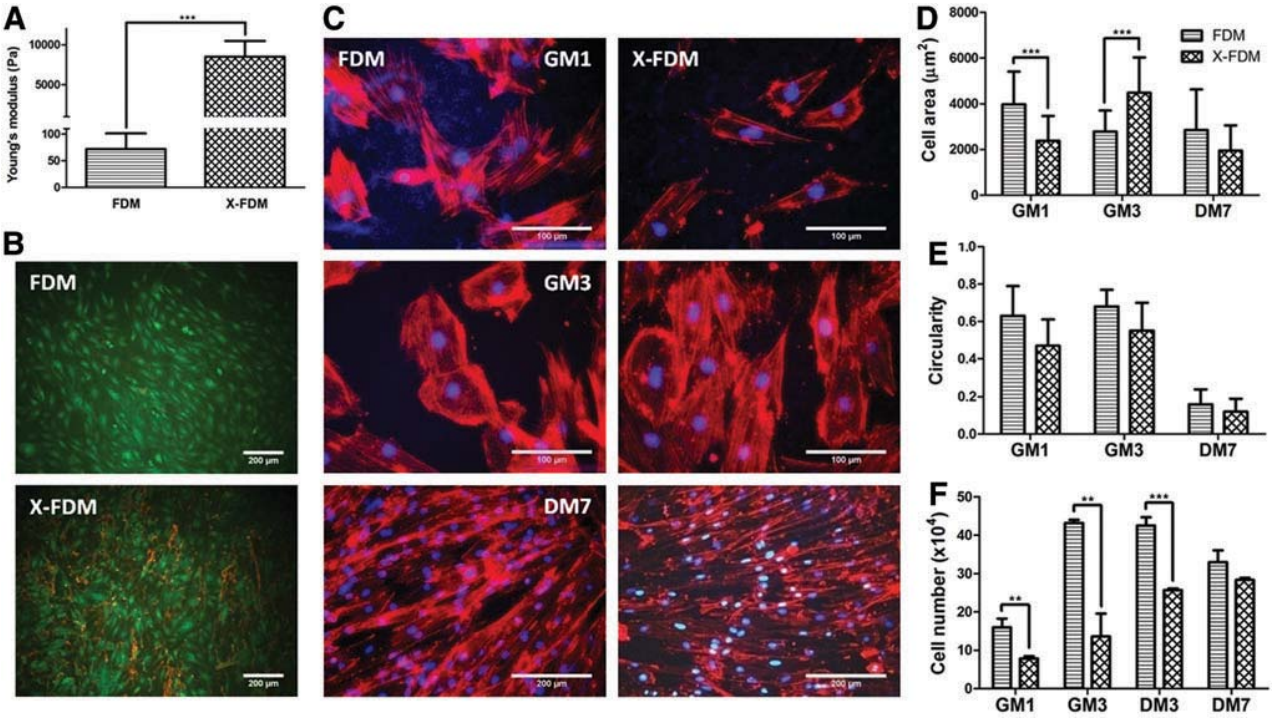

FIG. 6. **(A)** Substrate stiffness defined as Young's modulus for FDM and crosslinked FDM (X-FDM). **(B)** Cell viability assay of H9c2 cardiomyoblasts cultured on FDM and X-FDM for 24 h in GM; viable cells (*green*) and dead cells (*red*). *Orange color* in X-FDM is an autofluorescence of X-FDM under *blue* light filter in a fluorescence microscope. Scale bars are 200 μm. **(C)** F-actin (*red*) staining of H9c2 on FDM and X-FDM and nuclei stained with DAPI (*blue*). Scale bars are 100 μm (GM1 and GM3) and 200 μm (DM7). **(D, E)** Quantitative analysis of cell area and circularity based on IFS image analysis using ImageJ. **(F)** H9c2 proliferation assay on FDM and X-FDM. Statistical significance ($^{**}p < 0.01$ and $^{***}p < 0.001$). Color images available online at www.liebertpub.com/tea

assay in the GM condition found that while the cell number on FDM climbed significantly at GM3, on X-FDM was much smaller and rather constant with time (Fig. 6F). Interestingly, as the medium was switched to DM after 3 days of culture in GM (GM3), cell proliferation was very active on X-FDM at DM3, but stable on FDM at the same condition.

In addition, we have also investigated H9c2 cell adhesion on FDM and X-FDM through analysis of focal adhesion molecule (vinculin) and gene expression of α5 and β1 integrins. IFS staining of vinculin and F-actin, after cultured for 24 h in GM, shows that each cell on FDM has a significantly larger area of vinculin and a greater amount of focal adhesion molecule compared to that on X-FDM (Fig. 7A–C). To provide a further insight on cell adhesion, when gene expression of α5 and β1 integrin subunits was evaluated, the expression of α5 was significantly upregulated on FDM compared to that on X-FDM, but no appreciable difference was observed for β1 (Fig. 7D). In a parallel study, induction of cardiomyogenic differentiation of H9c2 cells at DM7 was also carried out using FDM and X-FDM. Cardiomyogenic protein markers, α-actinin and cTnT, were positively stained for both groups (Fig. 8A, B). Interestingly enough, quantitative assessment proved that much more positive signals were detected on X-FDM compared to those on FDM (Fig. 8C); the percentages of α-actinin and cTnT-positive nuclei were 2.2- and 1.6-fold higher, respectively, with X-FDM than with FDM and the difference was statistically significant.

Discussion

ECM with its unique biophysical and biomechanical properties would provide an excellent microenvironment for cell adhesion, proliferation, and differentiation. Previous works in our group showed that CDM, especially FDM, was very efficient for MSC differentiation into osteogenesis *in vitro*.[22] In another study using human umbilical vein endothelial cells, both FDM and preosteoblast-derived matrix were excellent in forming an assembly of capillary-like structure and in inducing a significant matrix remodeling for vasculogenesis.[23] Those experiences have prompted us to explore the potential of FDM as a novel culture platform for H9c2 cardiomyoblasts; a cell line isolated from embryonic rat heart tissue described in length by Hescheler *et al.*[16] In fact, many studies have shown that ECM plays a significant role in cardiomyocyte differentiation.[5,24,25] Hence, in this study, we have investigated the benefits of FDM in cellular behaviors of H9c2 cardiomyoblasts, primarily focusing on their differentiation into cardiomyogenic cells. H9c2 cells were used to provide an initial assessment of FDM on cardiomyogenesis for the following reasons: (1) H9c2 cells, while a cell line, are widely accepted as a model for cardiomyogenic differentiation and (2) the homogenous nature

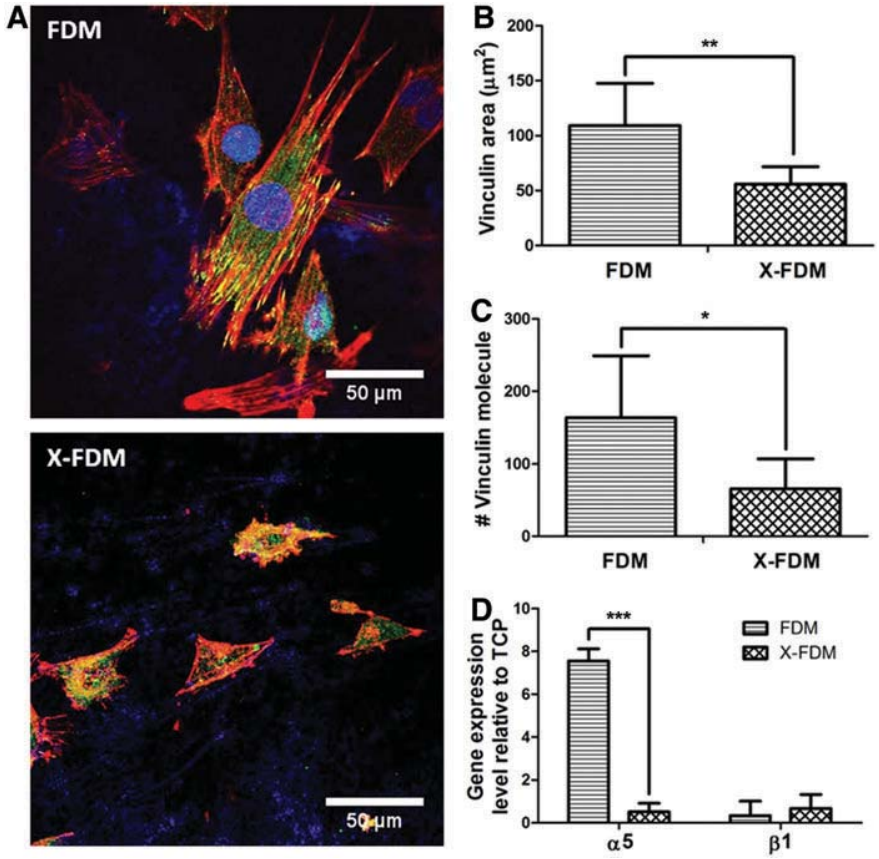

FIG. 7. Focal adhesion (FA) and integrin expression analysis of H9c2 cardiomyoblasts on FDM and X-FDM after 24 h of culture in growth medium. **(A)** IFS of vinculin (*green*) and F-actin (*red*) with nuclei stained by DAPI (*blue*). Scale bars = 50 μm. **(B, C)** Quantitative analysis of FA area and amount of vinculin per cell based on IFS image analysis using ImageJ. **(D)** Gene expression level of integrin subunits, α5 and β1, normalized to that of the cells cultured on TCP. Statistical significance (*$p < 0.05$, **$p < 0.01$, and ***$p < 0.001$). Color images available online at www.liebertpub.com/tea

of H9c2 cells, relative to primary cells, allows us to clearly delineate the effect of FDM and modified FDM (X-FDM) on cardiomyogenesis. As documented in this study with multiple results, FDM can be a useful platform toward cardiomyocyte differentiation of H9c2 compared to the common ECM materials, such as gelatin and fibronectin.

The differentiation of H9c2 cardiomyoblasts into cardiomyocytes was primarily confirmed by using IFS and gene expression. Stained against antibodies of α-actinin and

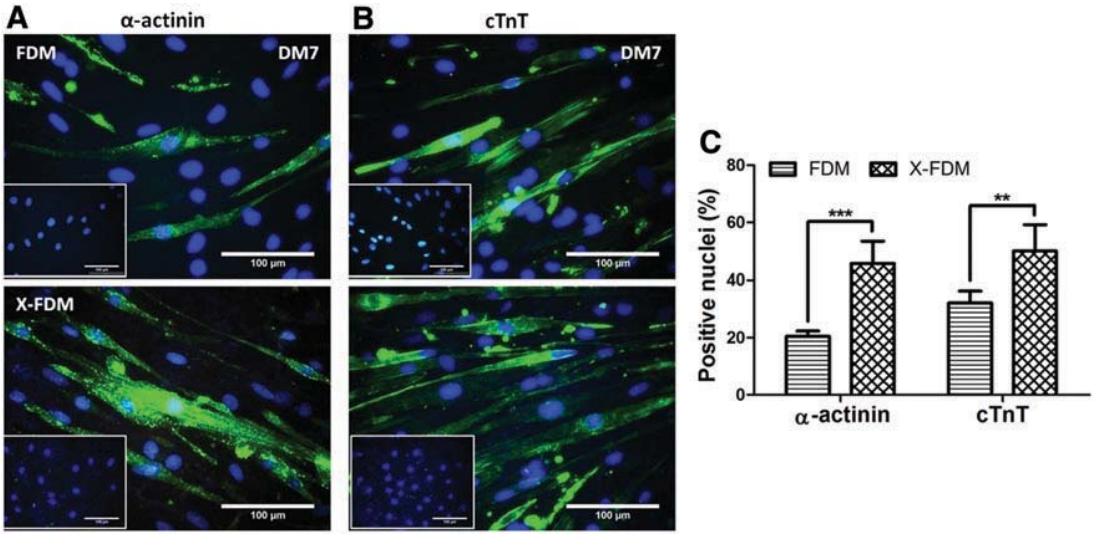

FIG. 8. H9c2 cardiomyoblast differentiation into cardiomyocytes on FDM and X-FDM at DM7. **(A)** IFS of α-actinin and **(B)** cTnT (both shown in *green*), along with nuclei stained with DAPI (*blue*). *Insets* show the cells before the induction of differentiation at GM3. **(C)** Quantitative analysis of nuclei positive for α-actinin and cTnT based on IFS image analysis using ImageJ. Data collected from five random IFS images. Statistical significance (**$p < 0.01$ and ***$p < 0.001$). Color images available online at www.liebertpub.com/tea

cTnT, the differentiated H9c2 exhibited positive signals the same to those observed on primary cardiomyocytes. Besides α-actinin and cTnT, another important protein in cardiac cells is connexin, which gives rise to a gap junction for intercellular communication through electrical and metabolic coupling between adjacent cells.[26] Cx43 is the major component of gap junction proteins in the heart that is developmentally regulated. During the embryonic stage of mouse cardiomyocytes, the expression of Cx43 increases as the developmental step proceeds,[27] indicating the critical role of this protein for cell maturation and function of synchronized beating. An upregulated expression of Cx43 is also correlated to the promotion of muscle differentiation in C2C12 myoblast.[28] The results (Fig. 5) display that before the cardiomyogenic induction, some cell populations are Cx43 positive, even in the GM condition (GM3), indicating that these cells are cardiac tissue origin. Another reason seems that given substrates may prime the cells for cardiac differentiation by increasing Cx43 expression at GM3 (Fig. 5C). Cells on FDM present a much advanced level of Cx43-positive cells at GM3 compared to that of gelatin and fibronectin, and the percentage continuously increases with FDM and fibronectin in DM7. Interestingly, H9c2 cardiomyoblasts on gelatin were rather constant in the expression level of Cx43 even in the differentiation medium condition.

However, one important feature that is missing from differentiated H9c2 is the formation of sarcomeric structure. This may explain the lack of beating activity of the resulting cardiomyocytes. In addition, even with a significantly increased gene expression related to cell contraction (Myl2 and Tnnt)[29,30] on FDM, it seems that current upregulation of such genes is insufficient to prove functional contractility of differentiated H9c2. Information about Myl2 protein expression that is lacked in this study might give a better insight, along with cTnT expression as shown in Figure 3. Many researchers have been unsuccessful in differentiating H9c2 into functional cardiomyocytes.[17,20] Therefore, while functional tests are critical, they are not a major focus in the current investigation. Because the contractility of cardiomyocytes is related to L-type calcium channels and connexin 43 (Cx43),[31] an upregulated level of Cx43 on the FDM might indirectly implicate cardiac functionality.

It is generally accepted that the importance of ECM is due mainly to the fact that ECM directly interacts with cells and controls their fate through modulating such properties, that is, matrix structure, matrix elasticity, matrix composition, and matrix-reserved growth factors.[6,32] It is also well known that cells have the ability to sense micro- and even nanoscale geometric cues from their microenvironments and as a result, presentation of specific matrix cue is extremely critical to properly manipulate a cell differentiation pathway.[33,34] The current FDM model holds multiple intrinsic cues at a time, clearly distinguished from gelatin or fibronectin. For example, as the FDM contains fibronectin, collagen I, and laminin, this combined ECM component may present a huge impact on how cells differentiate.[35] In fact, the ECM components are not restricted to these proteins; there are more in FDM, including vitronectin and collagen II and IV,[22] and other minor components such as perlecan, fibulin-2, and emilin-1 (data not published). Another cue is a unique surface topography due to the fibrillar structure of FDM compared to very smooth gelatin and fibronectin. Surface topography would provide an advanced microenvironment for maintenance of differentiated state of cardiomyocyte[36] and also a regulatory cue in stem cell differentiation.[37]

All of these innate properties of FDM give improved cell behaviors compared to those on gelatin or fibronectin. It is notable that direct comparison of FDM- and ECM-coated substrates would be difficult, because FDM is significantly different from those in their intrinsic properties (e.g., ligand density, substrate thickness, and stiffness). For example, the stiffness of gelatin and fibronectin is much greater than that of FDM (Fig. 1C). Indeed, given the multifaceted nature of cell-derived ECM, it is very challenging to control a single parameter of ECM. Despite such challenges, early studies that focus on a single ECM protein to investigate the role on cellular behavior are too limited and simplified in mimicking a natural cellular ECM microenvironment where various biochemical components are interactive with each other. Recently, combinatorial effects of multiple ECM proteins (Col I, FN, and Col IV) were investigated for human embryonic stem cell (hESC) differentiation in a 3D hydrogel form.[38]

Another interesting finding in this study is that H9c2 differentiation is further improved with the changes of substrate stiffness. We have tested the effect of crosslinking on matrix stiffness of FDM if matrix stiffness control would provide an additional advantage to the current system. The genipin-crosslinked FDM significantly increased the average stiffness of FDM up to 8.5 kPa, which corresponds to the reported stiffness for myogenic differentiation of naive MSCs.[39] Once genipin was chosen as a crosslinking agent due to its lower cytotoxicity,[40] our results (Fig. 6) indicate that except matrix stiffness, the crosslinked FDM is not much different with noncrosslinked FDM in terms of cell viability and morphology. On the other hand, the suppressed proliferation for cells on X-FDM gives another favorable correlation in increasing cell differentiation as mentioned earlier. As a result, enhanced matrix stiffness becomes a great advantage in inducing cardiomyogenic differentiation compared to rather soft matrix. Although there is a report that substrate stiffness could affect MSC fate,[39] current finding is the first to demonstrate cardiomyogenic differentiation of H9c2 cardiomyoblasts, in which matrix stiffness is a major contributor.

It should be, however, addressed that since H9c2 are not primary cells, it is of particular interest to evaluate how the current data are applicable to primary cardiac cells. Validating the present results using primary cardiac progenitors should provide a greater insight into the clinical relevance of FDM and X-FDM. Preliminary works in our group showed excellent cell adhesion of neonatal rat-derived cardiomyocytes and hESC-derived cardiomyocytes onto FDM (data not shown). In addition, compared to Matrigel, a stronger expression of cardiomyocyte-specific maker (cTnT) was observed with the hESC-derived cardiomyocytes cultured on the matrix in a defined condition. We anticipate that further comprehensive studies will make clear the role of varying matrix properties (e.g., natural and crosslinked) on the improvement of hESC-derived cardiomyocyte differentiation and functionality.

The mechanism behind such FDM performances for cardiomyogenic differentiation would have huge implications in cardiac tissue engineering. Indeed, while many previous studies using different cell types have reported the

positive effects of CDM, few show the exact mechanism in a comprehensive manner. Rather, many features of ECM (e.g., composition, topography, stiffness) have been examined separately.[35,37] Since this study indicated the impact of matrix stiffness on cardiomyogenesis, a mechanosensing-related target (i.e., nonmuscle myosin II) can be a major interest in the future work. It is speculated that as matrix stiffness increases, cells alter the nonmuscle myosin expression to produce greater forces on the actin cytoskeleton, which would be necessary to deform a stiffer matrix.[39] Cell adhesion is a very early cell behavior making specific interactions between the cell and ECM. Vinculin is one of the focal adhesion (FA) proteins that are connected to the actin cytoskeleton and deliver cell adhesion-related signals to the nucleus. Because expression of integrin and vinculin often correlates in a linear relationship,[41] studying integrin and vinculin expression would be a first step to understand how the cells sense microenvironments with different matrix stiffnesses.

Results at GM1 (Figs. 6D and 7B) present a correlation between the cell area and vinculin assembly; larger cell spreading increases the vinculin area.[42] Interestingly, the vinculin assembly for cells on X-FDM is much lower than those on FDM, which indicates a less cell–matrix interaction. It is interesting to note a recent study showing the relationship between FA molecules and cardiomyocytes using a simple model[43]; as two cardiomyocytes become mature, the level of FA expression decreases, thereby indicating that cell–cell interactions are becoming dominant, while the cell-ECM interactions are turning minor. Hence, the less cell–matrix interaction for cells on X-FDM may even further help the maturation state on the resulting cardiomyocytes. Since cell–matrix interaction is mainly through integrin binding to ECM, upregulated vinculin assembly on FDM is explained by a higher $\alpha 5$ integrin level[41] compared to that on X-FDM, even though another integrin subunit, $\beta 1$, shows little difference between the two groups.

In addition, cell geometry is another factor that can affect cell commitment to a certain lineage.[44] Specifically, H9c2 morphology has demonstrated to affect H9c2 behavior and differentiation.[20,45] Furthermore, it has shown that immature cardiomyocytes are circular in morphology, while mature cells are rod shaped.[46] From this perspective, we have looked at cell morphology as one potential parameter in assessing the cellular responses on different microenvironments. It seems that current results are premature to claim a strong correlation between morphological features and cell differentiation.

Conclusions

In this study, we have investigated the feasibility of FDM as a promising ECM platform for the induction of cardiomyogenic differentiation of H9c2 cardiomyoblasts. Based on the current data, FDM with its unique intrinsic properties (component, topography, stiffness) can give rise to a microenvironment that supports much improved differentiation and maturation capability of H9c2 cardiomyoblasts over gelatin or fibronectin. Interestingly, H9c2 cardiomyoblast differentiation was very sensitive in response to the change of matrix stiffness, preferring a stiffer matrix microenvironment. Our work suggests that FDM has a great potential as a tunable ECM platform to study cardiomyogenesis compared to conventional gelatin or fibronectin substrates.

Acknowledgments

This work was supported by an intramural grant 2V03350 (KIST) from the Ministry of Science, ICT, and Future Planning, Republic of Korea, and by a grant (A120216) of the Korean Health Technology R&D Project, Ministry of Health & Welfare, Republic of Korea.

Disclosure Statement

The authors have no potential conflicts of interest.

References

1. Hansson, E.M., Lindsay, M.E., and Chien, K.R. Regeneration next: toward heart stem cell therapeutics. Cell Stem Cell **5,** 364, 2009.
2. Burridge, P.W., Thompson, S., Millrod, M.A., Weinberg, S., Yuan, X., Peters, A., Mahairaki, V., Koliatsos, V.E., Tung, L., and Zambidis, E.T. A universal system for highly efficient cardiac differentiation of human induced pluripotent stem sells that eliminates interline variability. PLoS One **6,** e18293, 2011.
3. Lian, X. Directed cardiomyocyte differentiation from human pluripotent stem cells by modulating Wnt/Î²-catenin signaling under fully defined conditions. Nat Protoc **8,** 162, 2013.
4. Minami, I., Yamada, K., Otsuji, T.G., Yamamoto, T., Shen, Y., Otsuka, S., Kadota, S., Morone, N., Barve, M., Asai, Y., Tenkova-Heuser, T., Heuser, J.E., Uesugi, M., Aiba, K., and Nakatsuji, N. A small molecule that promotes cardiac differentiation of human pluripotent stem cells under defined, cytokine- and xeno-free conditions. Cell Rep **2,** 1448, 2012.
5. Zhang, J., Klos, M., Wilson, G.F., Herman, A.M., Lian, X., Raval, K.K., Barron, M.R., Hou, L., Soerens, A.G., Yu, J., Palecek, S.P., Lyons, G.E., Thomson, J.A., Herron, T.J., Jalife, J., and Kamp, T.J. Extracellular matrix promotes highly efficient cardiac differentiation of human pluripotent stem cells: the matrix sandwich method. Circ Res **111,** 1125, 2012.
6. Kleinman, H.K., Philp, D., and Hoffman, M.P. Role of the extracellular matrix in morphogenesis. Curr Opin Biotechnol **14,** 526, 2003.
7. Hynes, R.O. The extracellular matrix: not just pretty fibrils. Science **326,** 1216, 2009.
8. Ott, H.C. Perfusion-decellularized matrix: using nature's platform to engineer a bioartificial heart. Nat Med **14,** 213, 2008.
9. Flynn, L.E., Prestwich, G.D., Semple, J.L., and Woodhouse, K.A. Proliferation and differentiation of adipose-derived stem cells on naturally derived scaffolds. Biomaterials **29,** 1862, 2008.
10. Lu, H., Hoshiba, T., Kawazoe, N., Koda, I., Song, M., and Chen, G. Cultured cell-derived extracellular matrix scaffolds for tissue engineering. Biomaterials **32,** 9658, 2011.
11. Wolchok, J.C., and Tresco, P.A. The isolation of cell derived extracellular matrix constructs using sacrificial open-cell foams. Biomaterials **31,** 9595, 2010.

12. Narayanan, K., Leck, K.J., Gao, S., and Wan, A.C.A. Three-dimensional reconstituted extracellular matrix scaffolds for tissue engineering. Biomaterials **30,** 4309, 2009.
13. Paguirigan, A., and Beebe, D.J. Gelatin based microfluidic devices for cell culture. Lab Chip **6,** 407, 2006.
14. Li, M., Guo, Y., Wei, Y., MacDiarmid, A.G., and Lelkes, P.I. Electrospinning polyaniline-contained gelatin nanofibers for tissue engineering applications. Biomaterials **27,** 2705, 2006.
15. Ohashi, T., Kiehart, D.P., and Erickson, H.P. Dynamics and elasticity of the fibronectin matrix in living cell culture visualized by fibronectin–green fluorescent protein. Proc Nat Acad Sci USA **96,** 2153, 1999.
16. Hescheler, J., Meyer, R., Plant, S., Krautwurst, D., Rosenthal, W., and Schultz, G. Morphological, biochemical, and electrophysiological characterization of a clonal cell (H9c2) line from rat heart. Circ Res **69,** 1476, 1991.
17. Menard, C., Pupier, S., Mornet, D., Kitzmann, M., Nargeot, J., and Lory, P. Modulation of L-type calcium channel expression during retinoic acid-induced differentiation of H9C2 cardiac cells. J Biol Chem **274,** 29063, 1999.
18. Comelli, M., Domenis, R., Bisetto, E., Contin, M., Marchini, M., Ortolani, F., Tomasetig, L., and Mavelli, I. Cardiac differentiation promotes mitochondria development and ameliorates oxidative capacity in H9c2 cardiomyoblasts. Mitochondrion **11,** 315, 2011.
19. Sumi, D., Abe, K., and Himeno, S. Arsenite retards the cardiac differentiation of rat cardiac myoblast H9c2 cells. Biochem Biophys Res Commun **436,** 175, 2013.
20. Anene-Nzelu, C.G., Choudhury, D., Li, H., Fraiszudeen, A., Peh, K.Y., Toh, Y.C., Ng, S.H., Leo, H.L., and Yu, H. Scalable cell alignment on optical media substrates. Biomaterials **34,** 5078, 2013.
21. Subbiah, R., Ramasundaram, S., Du, P., Hyojin, K., Sung, D., Park, K., Lee, N.E., Yun, K., and Choi, K.J. Evaluation of cytotoxicity, biophysics and biomechanics of cells treated with functionalized hybrid nanomaterials. J R Soc Interface **10,** 6, 2013.
22. Bae, S.E., Bhang, S.H., Kim, B.S., and Park, K. Self-assembled extracellular macromolecular matrices and Their different osteogenic potential with preosteoblasts and rat bone marrow mesenchymal stromal cells. Biomacromolecules **13,** 2811, 2012.
23. Du P., Subbiah, R., Park, J.H., and Park, K. Vascular morphogenesis of human umbilical vein endothelial cells on cell-derived macromolecular matrix microenvironment. Tissue Eng Part A **20,** 2365, 2014.
24. Dijk, A., Niessen, H.W.M., Zandieh Doulabi, B., Visser, F.C., and Milligen, F.J. Differentiation of human adipose-derived stem cells towards cardiomyocytes is facilitated by laminin. Cell Tissue Res **334,** 457, 2008.
25. Jose, A., Santiago, R.P., and Ogle, B.M. Heterogeneous differentiation of human mesenchymal stem cells in response to extended culture in extracellular matrices. Tissue Eng Part A **15,** 3911, 2009.
26. van Veen, T.A.B., van Rijen, H.V.M., and Opthof, T. Cardiac gap junction channels: modulation of expression and channel properties. Cardiovasc Res **51,** 217, 2001.
27. Fromaget, C., Aoumari, A.E., and Gros, D. Distribution pattern of connexin 43, a gap junctional protein, during the differentiation of mouse heart myocytes. Differentiation **51,** 9, 1992.
28. Squecco, R., Sassoli, C., Nuti, F., Martinesi, M., Chellini, F., Nosi, D., Zecchi-Orlandini, S., Francini, F., Formigli, L., and Meacci, E. Sphingosine 1-phosphate induces myoblast differentiation through Cx43 Protein Expression: A role for a gap junction-dependent and -independent Function. Mol Biol Cell **17,** 4896, 2006.
29. Ares-Carrasco, S., Picatoste, B., Camafeita, E., Carrasco-Navarro, S., Zubiri, I., Ortiz, A., Egido, J., López, J.A., Tuñón, J., and Lorenzo, O. Proteome changes in the myocardium of experimental chronic diabetes and hypertension: Role of PPARα in the associated hypertrophy. J Proteomics **75,** 1816, 2012.
30. Rottbauer, W., Wessels, G., Dahme, T., Just, S., Trano, N., Hassel, D., Burns, C.G., Katus, H.A., and Fishman, M.C. Cardiac myosin light chain-2: a novel essential component of thick-myofilament assembly and contractility of the heart. Circ Res **99,** 323, 2006.
31. Cui, H., Liu, Y., Cheng, Y., Zhang, Z., Zhang, P., Chen, X., and Wei, Y. *In vitro* study of electroactive tetraaniline-containing thermosensitive hydrogels for cardiac tissue engineering. Biomacromolecules **15,** 1115, 2014.
32. Reilly, G.C., and Engler, A.J. Intrinsic extracellular matrix properties regulate stem cell differentiation. J Biomech **43,** 55, 2010.
33. Guilak, F., Cohen, D.M., Estes, B.T., Gimble, J.M., Liedtke, W., and Chen, C.S. Control of stem cell fate by physical interactions with the extracellular matrix. Cell Stem Cell **5,** 17, 2009.
34. Dalby, M.J. The control of human mesenchymal cell differentiation using nanoscale symmetry and disorder. Nat Mater **6,** 997, 2007.
35. Flaim, C.J., Chien, S., and Bhatia, S.N. An extracellular matrix microarray for probing cellular differentiation. Nat Meth **2,** 119, 2005.
36. Polonchuk, L., Elbel, J., Eckert, L., Blum, J., Wintermantel, E., and Eppenberger, H.M. Titanium dioxide ceramics control the differentiated phenotype of cardiac muscle cells in culture. Biomaterials **21,** 539, 2000.
37. Chen, G.Y., Pang, D.W.P., Hwang, S.M., Tuan, H.Y., and Hu, Y.C. A graphene-based platform for induced pluripotent stem cells culture and differentiation. Biomaterials **33,** 418, 2012.
38. Yang, F., Cho, S.-W., Son, S.M., Hudson, S.P., Bogatyrev, S., Keung, L., Kohane, D.S., Langer, R., and Anderson, D.G. Combinatorial extracellular matrices for human embryonic stem cell differentiation in 3D. Biomacromolecules **11,** 1909, 2010.
39. Engler, A.J., Sen, S., Sweeney, H.L., and Discher, D.E. Matrix elasticity directs stem cell lineage specification. Cell **126,** 677, 2006.
40. Koo, H.J., Song, Y.S., Kim, H.J., Lee, Y.H., Hong, S.M., Kim, S.J., Kim, B.C., Jin, C., Lim, C.J., and Park, E.H. Antiinflammatory effects of genipin, an active principle of gardenia. Eur J Pharmacol **495,** 201, 2004.
41. Gallant, N.D., Michael, K.E., and García, A.J. Cell adhesion strengthening: Contributions of adhesive area, integrin binding, and focal adhesion assembly. Mol Biol Cell **16,** 4329, 2005.
42. Chen, C.S., Alonso, J.L., Ostuni, E., Whitesides, G.M., and Ingber, D.E. Cell shape provides global control of focal adhesion assembly. Biochem Biophys Res Commun **307,** 355, 2003.
43. McCain, M.L., Lee, H., Aratyn-Schaus, Y., Kléber, A.G., and Parker, K.K. Cooperative coupling of cell-matrix and

cell–cell adhesions in cardiac muscle. Proc Nat Acad Sci USA **109,** 9881, 2012.
44. Kilian, K.A., Bugarija, B., Lahn, B.T., and Mrksich, M. Geometric cues for directing the differentiation of mesenchymal stem cells. Proc Nat Acad Sci USA **107,** 4872, 2010.
45. Pan, H.-A., Hung, Y.-C., Sui, Y.-P., and Huang, G.S. Topographic control of the growth and function of cardiomyoblast H9c2 cells using nanodot arrays. Biomaterials **33,** 20, 2012.
46. Yang, X., Pabon, L., and Murry, C.E. Engineering adolescence maturation of human pluripotent stem cell-derived cardiomyocytes. Circ Res **114,** 511, 2014.

Address correspondence to:
Kwideok Park, PhD
Center for Biomaterials
Korea Institute of Science and Technology
Seoul 136-791
Republic of Korea

E-mail: kpark@kist.re.kr

Received: October 14, 2014
Accepted: March 16, 2015
Online Publication Date: April 28, 2015